Computation of Bias on Measured α_p by Monte-Carlo Simulation

R. Boffy, C. Jammes

Computation of Bias on Measured α_{p} by Monte-Carlo Simulation

R. Boffy[1] **and C. Jammes**[1]
[1]CEA, DEN, DER, Instrumentation, Sensors and Dosimetry Laboratory
Cadarache, F-13108 Saint-Paul-lez-Durance, France

romain.boffy@cea.fr, christian.jammes@cea.fr

ABSTRACT

Controlling the reactivity of a nuclear reactor requires the knowledge of its kinetic parameters. Even though they can be computed by neutronic codes, they often have to be measured to finish the commissioning of a new installation. Amongst the list of kinetic parameters, we are specifically interested in the prompt-decay constant (α_{p}). In practice, the presence of a reflector generates a decay constant, which will differ from core's α_{p}, and that might disturb the measurement of the whole set of kinetic parameters. Such a behaviour is a drawback for experimentalists since neutron detectors are usually located in non-fissile areas. The aim of the study is to give numerical estimates of the bias that can come out when measuring kinetic parameters of a light-water nuclear reactor. The work is based on on time-impulse techniques to derive kinetic parameters from the flux decay of the system. The impact of the detector position, as well as the reactivity level have been studied in a concurrent way. As an example, it was shown that α_{p} could be underestimated by a factor ranging from 8 to 12 % in a case of a sub-criticality of -3600 pcm, if the detector was located in the core or the reflector, respectively.

KEYWORDS: Nuclear reactor , kinetic parameters , alpha, Monte-Carlo

1. INTRODUCTION

In view of the commissioning of the Jules-Horowitz Reactor [1], efforts are produced to estimate the bias that may appear when measuring the kinetic parameters of the reactor. Specifically, we are interested in the impact of detector's location on its response.
When studying heterogeneous neutronic systems, point kinetic theory allows predicting their time behaviour as several sets of kinetic parameters depending on where they are measured [2, 3]. The importance of detector's location is even more marked when the system dives into deep subcriticality. Practically, detectors located outside the core will measure kinetic parameters which depend on the materials of the reflector and their distance to the fissile region. It is possible to adjust measured values to account for the bias of a detector thanks to correction factors found by simulation. Such a technique has been applied on practical cases when measuring the kinetic parameters of specific nuclear systems [4, 5].
In the present study, we are interested in a thermal reactor with a simplified geometry so that it will be possible to estimate the bias that can appear when measuring kinetic parameters in different areas.

2. MATERIALS AND METHODS

2.1. Theoretical background

During a neutron-noise measurement, impulses are created by delayed neutrons and kinetic parameters can be found by studying correlations in the neutron signal. In this study, the time-impulse response is created by an external source and parameters are found from studying the flux decay curve. In our case, a pulsed neutron source is justified by the fact that we study the time decay constants and not the flux intensity itself.
In the case of sub-critical reactor, where point-kinetic equations are assumed as applicable as first approach, the flux intensity in the reactor can be described as a group of decaying exponentials [6]. The time constants of these functions can be extracted from the inhour equation. One of them being the prompt-decay constant, α_{p}, while the others depend on the delayed neutron precursor groups.

The prompt-decay constant can be derived by fitting the decay curve within the millisecond time-range with an exponential function: $b \cdot \exp^{-\alpha_{\mathrm{p}} t}$, b being a constant. If this procedure is repeated for different reactivity configurations, it is possible to derive the neutron-delayed fraction, β_{eff}, and the generation time, Λ, from the curve $\alpha_{\mathrm{p}}(\rho)$, since α_{p} = (β_{eff} - ρ) / Λ. During a neutron noise measurement campaign in a reactor, kinetic parameters are found by Rossi-α or Feynman-α technique. Bias appear in the values derived from the measurements and the present study will allow us to estimate them.

2.2. Reactor characteristics

To study the effect of detectors' positions on measured kinetic parameters in a general configuration, the reactor geometry was kept relatively simple. It consists in a homogeneous cylindrical core composed UO_2 and H_2O, surrounded by a light water reflector, also cylindrical. One control and two safety rods were added in the core region. Practically, the safety rods volumes were left empty while, while in the control rod the limit between absorbing material and void was varied. An empty channel was added in the lower part of the reflector to feed the core by an external source. Finally, five empty spaces were added to simulate the presence of neutron noise detectors. Two cross-sections of the reactor are reported in Fig.1.

The composition of the different materials are gathered in Table 1. The proportion of the different elements has been chosen to be close to the one of PWR.

The external source was located in the feeding channel. The initial orientation of the neutrons was set parallel to the Z-axis and without angular divergence. That way, the first material encountered by incident neutrons is the core. A Watt fission spectrum was chosen as initial energy distribution.

In terms of geometry, the reactor has a cylindrical shape with equal height and diameter. For the core and reflector they are 66 cm and 120 cm, respectively. The volumes simulating safety and control rods have 16 cm of diameter and are 66 cm high. The geometry has been set in order to reach delayed criticality for a control rod insertion around 25 %.

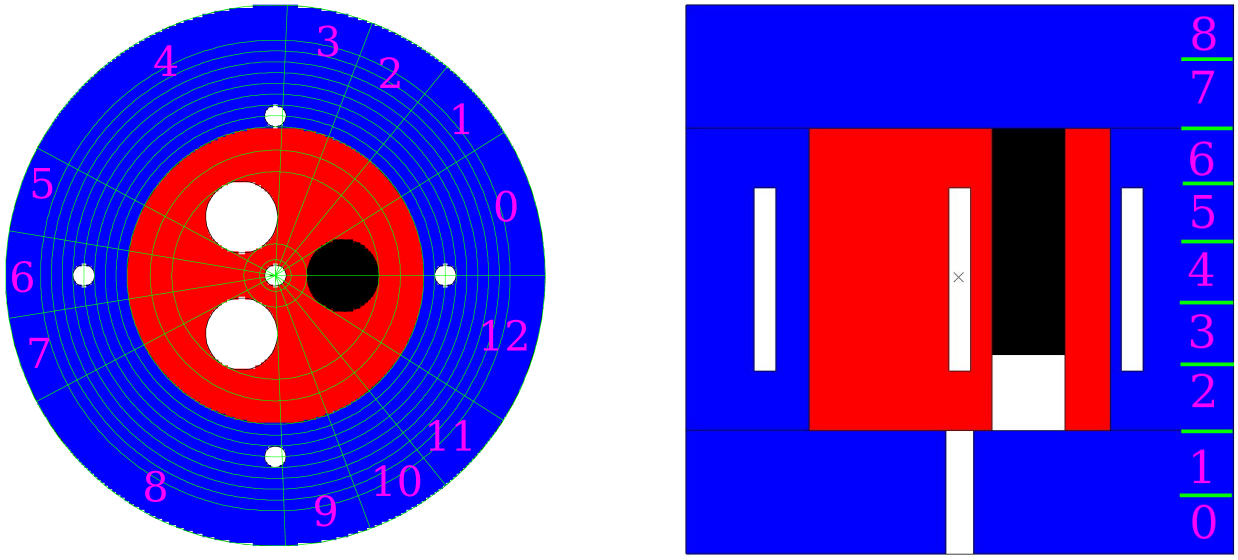

(a) (b)

Figure 1: Cut views perpendicular to Z-axis (a) and Y-axis (b) at the centre of the reactor. Colors correspond as follows: red to the fuel, blue to the reflector, black to the absorber, and white to void. Green lines are the mesh tally on view (a). Solely an outline of the z-mesh is drawn on Fig. (b). Numbers correspond to θ and z binning used when plotting results.

Table 1: Material composition of simulated reactor

Element	U-235	U-238	B10	B11	C	H	O
Core	0.56 %	10.56 %	-	-	-	44.44 %	44.44 %
Reflector	-	-	-	-	-	33 %	66 %
Absorber	-	-	15.92 %	64.08 %	20 %	-	-
Void	$= 1 \times 10^{-16}$ at/cm^3						

2.3. Simulation programs

The Monte-Carlo transport code TRIPOLI-4® [7] has been used for this study. Kinetic parameters obtained in criticality mode were used as reference to the values obtained in fixed source mode. The control rod insertion was varied from 25 % to 100 %.

In fixed-source mode, each source neutron was generated $t = 0$ s and the induced flux in the reactor was monitored as a function of the time. Particles were tracked thanks to a mesh tally that covered the whole system. To fit the reactor geometry, the mesh tally had a cylindrical shape with limits corresponding to the different cells. As an example, Fig. 1a shows the arrangement of the

mesh in the horizontal section. One can see that it depends on the distance from the centre and that it is sliced angularly with respect to the safety and control rods. The mesh on the vertical section has not been displayed on Fig. 1b because of the difficulty to represent the superposition of horizontal and tangential limits. Only an outline of the z-mesh is drawn on that latter figure.

2.4. Data treatment

Flux decay of the reactor could be either monitored in some specific cells, such as the empty ones representing noise-detection chambers, or all across the system thanks to the mesh mentioned earlier. The results presented here were generated with that latter technique in order to analyse the spatial dependence of the measured kinetic parameters.

Figures 2a and 2b show the flux decay in logarithmic and semi-logarithmic scale, respectively. The time span of the latter figure is focused on the prompt decay duration. There, one can see from the linear decrease lines, the exponential nature of the prompt decay. Figure 2b allows to find the time limits for data fitting. z-bin number 2 corresponds the bottom of the core region, r-bin number 0 corresponds to the center while numbers 5 and 7 correspond the first and third reflector layers, respectively.

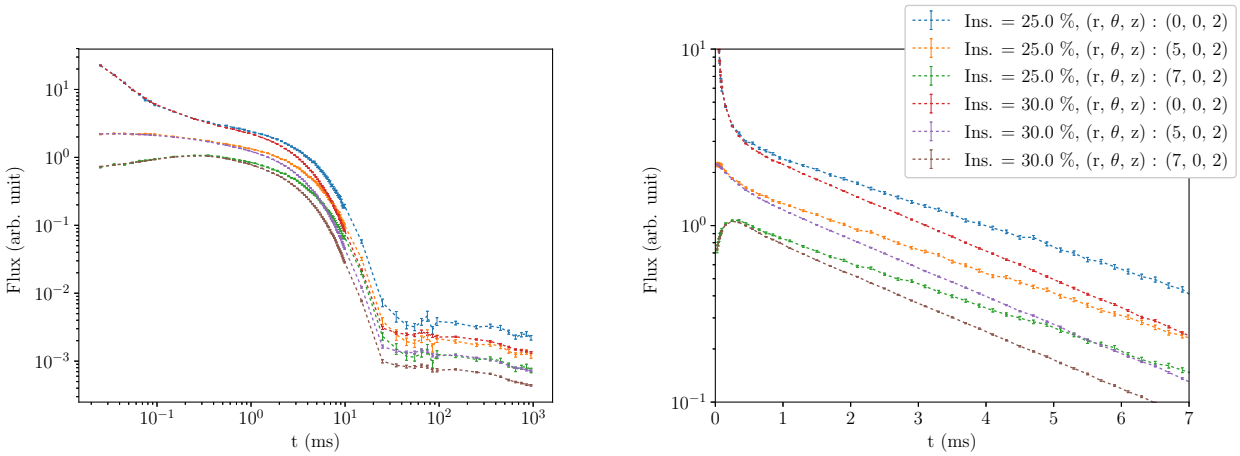

(a) **(b)**

Figure 2: Time-impulse response simulated by TRIPOLI-4, for 25 % and 30 % insertion of neutron absorber. Legend from Fig. (b) also apply to Fig. (a)

Then, decay curves were fitted by an exponential function, $b{\cdot}\exp^{-\alpha_p \cdot t}$, using a least-squares method (Python and SciPy library). Finally, the α_{p} parameters derived were compared to the ones obtained in criticality computations. In the next sections of this article, these constants are quoted $\alpha_{\mathrm{p}}^{\mathrm{meas.}}$ and $\alpha_{\mathrm{p}}^{\mathrm{crit.}}$, respectively.

3. RESULTS

3.1. Critical mode

Kinetic parameters given by TRIPOLI-4 when run in critical mode will serve as reference for the values derived in time-impulse configuration. Reactivity variation as a function of control rod insertion is shown in Fig. 3a. The prompt-decay constant computed from β_{eff} and Λ, which are directly given by the transport codes, is plotted as a function of the reactivity in Fig. 3b. One has to note that the error bars shown in both figures correspond to 1-σ uncertainty.

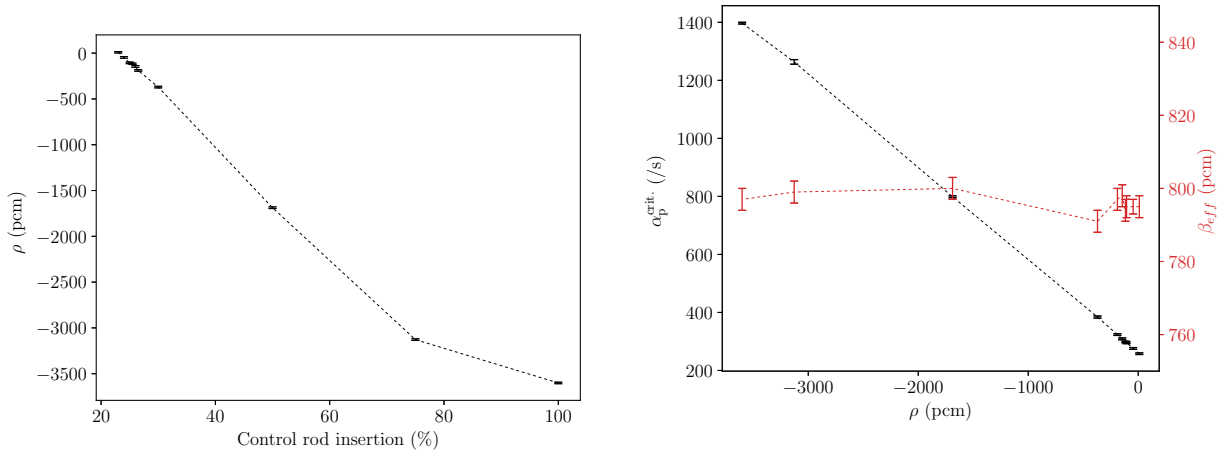

(a) Reactivity curve.

(b) Prompt-decay constant and effective delayed neutron fraction.

Figure 3: Critical mode simulation results.
Uncertainties on ρ on plot (b) are indistinguishable.

3.2. Fixed source mode

The derivation of $\alpha_{\text{p}}^{\text{meas.}}$ at different positions in the reactor are reported in Fig. 4 and 5 . More specifically, plots display the radial dependence for fixed z and θ. Values are compared to the one found in critical mode for the corresponding absorber insertion. The points corresponding to $r < 33$ cm are located in the core while the others are located in the reflector. The time-impulse analysis allows to find values very close to the critical-mode $\alpha_{\text{p}}^{\text{crit.}}$ as long as it is computed in the core and for slight sub-criticality. Once located in the reflector, the value is underestimated which is what was expected.

On Fig.4a, $\alpha_{\text{p}}^{\text{meas.}}(r)$ is plotted for different θ directions on the median section. One can see that in the core region there is no clear influence of the θ direction when the system is slightly sub-critical ($\rho \sim -100$ pcm). Once in the reflector, α_{p} is underestimated and this trend emphasise for curves further from the control rod area ($\theta > 0$). Concerning the z dependence, Fig. 4b, it appears that the distance to the source impacts slightly the derived $\alpha_{\text{p}}^{\text{meas.}}$ even in the core region. However, considering the uncertainties the effect is relatively negligible.

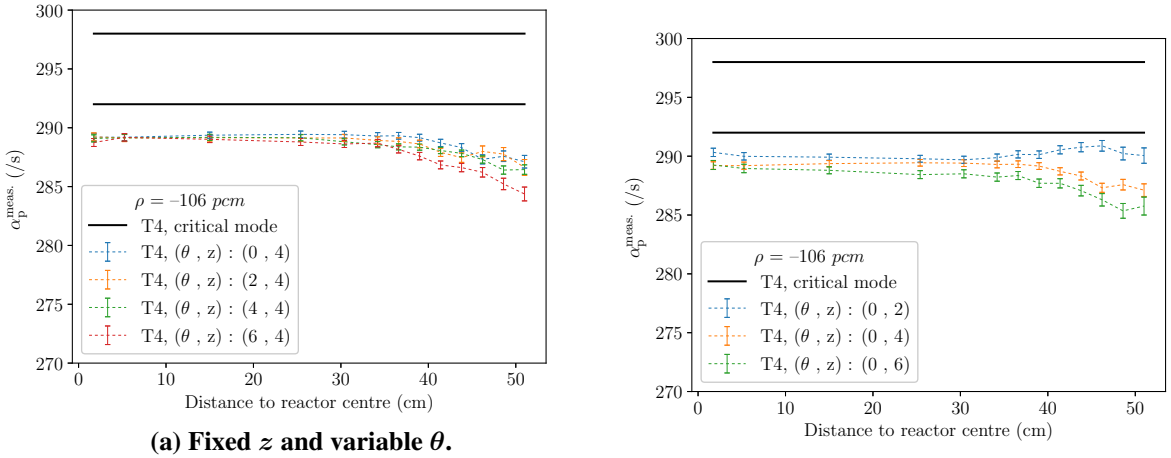

(a) Fixed z and variable θ.

(b) Fixed θ and variable z.

Figure 4: Prompt-decay constant by time-impulse fit for 25 % absorber insertion. Radial (b) and tangential (a) dependence.

Figure 5 shows fitting results when the system is deeply sub-critical ($\rho \sim -3600$ pcm). In addition to the remarks of the 25 % insertion case, one can see that even in the core, reference $\alpha_p^{crit.}$ value cannot be obtained with the time-impulse technique. Also, the measurement of $\alpha_p^{meas.}$ is getting worse as it is done deeper in the reflector. Considering the z dependence, see Fig. 5b, one can see that in the core, $\alpha_p^{meas.}$ is underestimating $\alpha_p^{crit.}$ as the measure is done further from the source. This kind of trend has to be expected in Accelerator-Driven Systems but not during a noise measurement because in that latter case the source neutrons are the delayed precursors and are located everywhere in the core.

4. ANALYSIS

4.1. Neutron decay rate in reflector

As can be seen from the different figures of the Results section, $\alpha_p^{meas.}$ values derived in the reflector tend to deviate from the ones obtained in critical mode. This is due to the absorptions in that region. The total flux response in reflector results from the core decay, characterized by α_p, and the reflector decay itself, characterized by the constant λ_r.

To isolate λ_r, the neutron current going from the core to the reflector was tallied as a function of the energy spectrum. This was used as a source for a reflector element (H_2O) of cylindrical shape. Neutrons were shot from one end and the decay was measured at different distances from that. Again, solely the shape of the decay interests us and not the intensity. The cylindrical side of the cell was set reflective in order to keep neutrons inside and propagate them in the volume. In the end, this corresponds to a 1-D problem.

Figure 6a shows the time decay curve at different distances from neutron entrance. Fitting those curves with an exponential allows to find λ_r. The analysis was done between 0.75 ms and 1.5 ms. Results are displayed in Fig. 6b. One can see that the neutron decay rate in the reflector is relatively

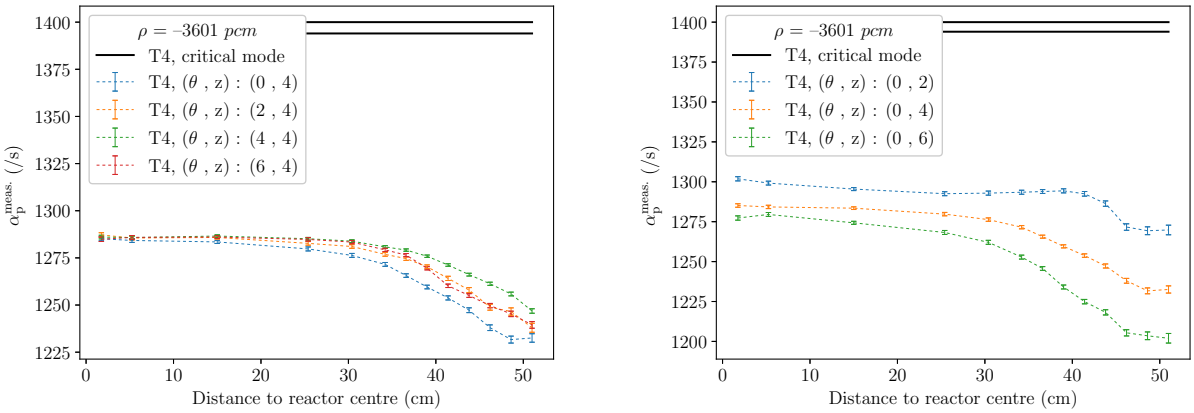

(a) Fixed z and variable θ. **(b) Fixed θ and variable z.**

Figure 5: Prompt-decay constant by time-impulse fit for 100 % absorber insertion. Tangential (a) and radial (b) dependence.

stable from 0 to 5 cm, at around 5600 /s, it then decreases at around -70 /s/cm until 35 cm to stabilize around 3800 /s, though that latter value shows relatively high uncertainties. The consequences of such results will be analysed in the light of the reactivity and corresponding α_{p}.

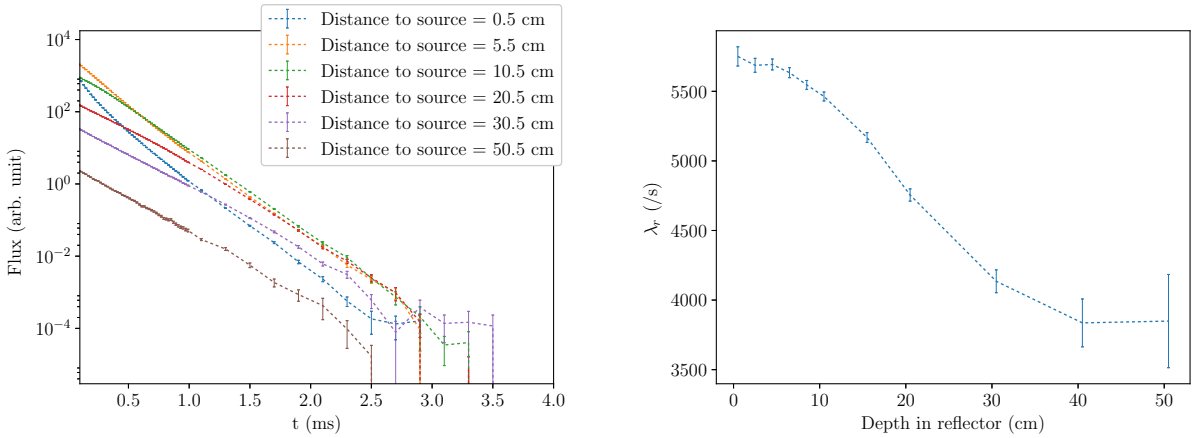

(a) Time decay for different depths. **(b) λ_r evolution in reflector.**

Figure 6: Time impulse response of the reflector when exposed to the spectrum exiting the core region.

4.2. Expected bias on measured prompt decay constant

Spriggs *et al.* clarified the Avery-Cohn theory on reflected reactors [2]. They defined the probability for a neutron to go from the core to the reflector or vice-versa: f_{cr} or f_{rc}, respectively. And

the product of these two probabilities as the *reflector return fraction*, $f = f_{cr} f_{rc}$. For such a system, the inhour equation involves the core prompt behaviour, the delayed neutrons source, and the neutrons returning from the reflector. In our case, since $\alpha_{\rm p}/\lambda_r \ll 1$, the root ($\omega$) corresponding to the prompt decay can be found by simplifying the inhour equation: $\omega = (\rho - \beta)/(\Lambda + f\Lambda_r)$. Where $\Lambda_r = 1/(\lambda_r k_{eff}(1-f))$ is the reflector's prompt generation time. The application of this formulae does not allow to forecast $\alpha_{\rm p}^{\rm meas.}$ since f is unknown. Though, having found $\alpha_{\rm p}^{\rm meas.}$ by time-impulse simulation, one can estimate f for different reactivity levels:

$$f = \frac{\alpha_p^{crit.} - \alpha_p^{meas.}}{\alpha_p^{crit.} - \alpha_p^{meas.} + \frac{\alpha_p^{meas.}}{\lambda_r k_{eff} \Lambda}} \tag{1}$$

Which yields, $f \approx 0.12$ for $\rho \approx -3600$ pcm, and $f \approx 0.026$ for $\rho \approx -100$ pcm. This highlights that the deep sub-critical case is greatly influenced by the reflector since around 12 % of neutrons are leaking to the reflector and returning in the core, while solely 2.6 % are following this route for the slightly critical configuration. This allows to understand why $\alpha_{\rm p}^{\rm meas.}$ is noticeably under $\alpha_{\rm p}^{\rm crit.}$ when the core is deeply subcritical, see Fig. 5a.

A simplification of that model is to consider that no neutron from the reflector will return in the core ($f_{rc} = 0$). Discarding the neutron source from precursors, for we are interested in the prompt-decay time range, one finds the number of neutrons in the reflector as:

$$N_r(t) = \lambda_{cr} N_0 \exp(-\lambda_r t) H(t) * \exp(-\alpha_{\rm p} t) H(t) \tag{2}$$

$$= \frac{\lambda_{cr} N_0}{\lambda_r - \alpha_p} \left(\exp(-\alpha_{\rm p} t) - \exp(-\lambda_r t)\right) \tag{3}$$

$H(t)$ being the Heavyside function, λ_{cr} the probability by time unit for a neutron from the core to go in the reflector, and N_0 the magnitude of the neutron burst at $t = 0$. The convolution of the two exponentials will induce a decrease of neutron density for short time scale where the reflector time period is dominant, while latter the decay will be driven by $\alpha_{\rm p}$. In fact, these trends can be seen in Fig. 2b for the $r = 7$ bin, below and above 0.5 ms, respectively.
The discrepancy between the measured decay constant and the core $\alpha_{\rm p}^{\rm crit.}$ can be estimated thanks to some approximations. Let us consider that $\alpha_{\rm p}^{\rm meas.}$ is obtained by curve fitting at $t \sim 1/\alpha_p$ and that we study the ratio of λ_r and $\alpha_{\rm p}$, *i.e.* we set $\lambda_r = k \cdot \alpha_p$. One estimates the measured decay constant $\alpha_p^{meas.}$ by deriving the logarithm Eq. 3:

$$\alpha_{\rm p}^{\rm meas.}(k) = \alpha_{\rm p}^{\rm crit.} \left(1 - \frac{k-1}{\exp(k-1) - 1}\right) \tag{4}$$

The evolution of $\alpha_{\rm p}^{\rm meas.}/\alpha_{\rm p}^{\rm crit.}$ as a function of k is shown on Fig 7. One can see that, depending upon k, which is proportional related to ρ, the measured prompt decay constant will drift from $\alpha_{\rm p}^{\rm crit.}$. Let us take the two extreme cases of insertions of 25 % and 100 % that correspond to 260 /s and 1400 /s, respectively. For the first case, we have $k \in [13; 20]$, depending upon the distance to the core, and this gives a ratio higher than 0.99. Looking at the curves on Fig. 4, it is what is observed for $z = 2$ whatever the distance to the core. In the case of $z = 6$, the maximum underestimation is 3 %. However, considering the uncertainty on $\alpha_{\rm p}^{crit.}$, one can say that the formulae is relatively good on that situation. For the deep-critical case, we have $k \in [3; 4]$, which should

correspond to a ratio $\in [0.69; 0.84]$. The worst case in the reflector gives a ratio around 0.88, and the value derived in the core is solely 0.92.
These latter results show that measurements in deep critical conditions are closer from reality than expected. However, we see that in-core measurements will be biased, though it is not forecast by the two-regions model with neutrons going solely from the core to the reflector. Anyhow, Eq. 4 allows to have a quick estimate of whether kinetic parameters measured in the reflector will be acceptable or not.

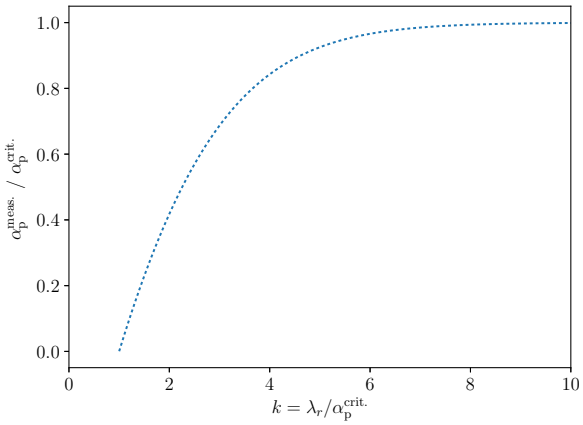

Figure 7: Under-estimation of α_{p} when measured in reflector. Case of a two-regions model with $f_{rc} = 0$, see Eq. 4.

5. CONCLUSIONS

This study allowed to evidence the bias on a measured α_{p} as a function of the position in the reactor and its criticality level. It was shown, in the reflector, that the measured α_{p} will drift below the critical value as getting further from the fissile region. This is especially true when α_{p} approaches the neutron lifetime in reflector, λ_r. Finally, simulations have shown that for deep critical configurations, *e.g.* $\rho \sim -3600$ pcm, α_{p} value measured in the core region underestimates the critical value because of the relatively important proportion of neutrons from the reflector returning in the core.

NOMENCLATURE

- α_{p}: prompt decay constant given in critical mode by TRIPOLI-4®
- $\alpha_{\mathrm{p}}^{\mathrm{crit.}}$: prompt decay constant computed by TRIPOLI-4 in critical mode.
- $\alpha_{\mathrm{p}}^{\mathrm{meas.}}$: prompt decay constant derived from time-impulse analysis.
- f_{cr} and f_{rc}: probability for a neutron to go from the core to the reflector and from the reflector to the core, respectively.
- $f = f_{cr} f_{rc}$: neutron return fraction.
- λ_r: neutron decay rate in reflector
- T4: TRIPOLI-4®

ACKNOWLEDGEMENTS

The authors would like to thank Dr Grégoire De Izarra and Dr Benoît Geslot for their assistance on the redaction of this article.

REFERENCES

[1] G. Bignan, C. Colin, J. Pierre, C. Blandin, C. Gonnier, M. Auclair, and F. Rozenblum. The jules horowitz reactor research project: A new high performance material testing reactor working as an international user facility - first developments to address r&d on material. In *MINOS 2$^{\mathrm{nd}}$ International Workshop, Irradiation of Nuclear Materials: Flux and Dose Effects*, volume 115, 2016. https://doi.org/10.1051/epjconf/201611501003.

[2] G. D. Spriggs, R. D. Busch, and J. G. Williams. Two-region kinetic model for reflected reactors. *Ann. Nucl. Energy*, 24(3):205–250, 1997.

[3] C. Jammes, B. Geslot, and G. Imel. Advantage of the area-ratio pulsed neutron source technique of ads reactivity calibration. *Nucl. Instr. and Meth. in Phys. Res. A*, 562:778–784, 2006.

[4] G. Perret, B. Geslot, A. Gruel, P. Blaise, J. Di-Salvo, G. De Izarra, C. Jammes, M. Hursin, and A. Pautz. Kinetic parameter measurements in the MINERVE reactor. *IEEE Transactions on Nuclear Science*, 64(1):724–734, 2017.

[5] A. Talamo, Y. Gohar, S. Sadovich, H. Kiyavitskaya, V. Bournos, Y. Fokov, and C. Routkovskaya. Correction factor for the experimental prompt neutron decay constant. *Ann. Nucl. Energy*, 62:421–428, 2013.

[6] K. O. Ott and R. J. Neuhold. *Introductory Nuclear Reactor Dynamics*. American Nuclear Society, 1985.

[7] E. Brun, F. Damian, C.M. Diop, E. Dumonteil, F.X. Hugot, C. Jouanne, Y.K. Lee, F. Malvagi, A. Mazzolo, O. Petit, J.C. Trama, T. Visonneau, and A. Zoia. TRIPOLI-4, CEA, EDF and AREVA Reference Monte-Carlo Code. *Annals of Nuclear Energy*, 82:151–160, 2015.